Chiral Ionic Liquids

International Edition: DOI: 10.1002/anie.201605792
German Edition: DOI: 10.1002/ange.201605792

Symmetry Breaking in Chiral Ionic Liquids Evidenced by Vibrational Optical Activity

Patric Oulevey, Sandra Luber, Birte Varnholt, and Thomas Bürgi*

Abstract: *Ionic liquids (ILs) are receiving increasing interest for their use in synthetic laboratories and industry. Being composed of charged entities, they show a complex and widely unexplored dynamic behavior. Chiral ionic liquids (CILs) have a high potential as solvents for use in asymmetric synthesis. Chiroptical methods, owing to their sensitivity towards molecular conformation, offer unique possibilities to study the structure of these chiral ionic liquids. Raman optical activity proved particularly useful to study ionic liquids composed of amino acids and the achiral 1-ethyl-3-methylimidazolium counterion. We could substantiate, supported by selected theoretical methods, that the achiral counterion adopts an overall chiral conformation in the presence of chiral amino acid ions. These findings suggest that in the design of chiral ionic liquids for asymmetric synthesis, the structure of the achiral counter ion also has to be carefully considered.*

Ionic liquids (ILs) are subject of high interest owing to their potential applications, for example, as electrolytes, in catalysis, and as green solvents, and experience a revival that began more than two decades ago.[1–9] The main difference with respect to conventional organic solvents is their almost non-existent vapor pressure as a result of the strong interactions between anions and cations. The characterization of ILs and understanding the consequences of the strong interactions on the structural properties is a challenge, both experimentally[10] and theoretically.[11]

Chiral ionic liquids (CILs) play an important role, for example, in asymmetric synthesis.[12–19] Herein, we focus on such CILs consisting of L or D enantiomers of the amino acid anions alanine (Ala), valine (Val), or leucine (Leu) in combination with the widely used positively charged 1-ethyl-3-methylimidazolium (Emim) as counterion. These CILs have been obtained from ion exchange synthesis of a [Br][Emim] salt[13] and will be referred to as [Ala][Emim], [Val][Emim], and [Leu][Emim], respectively. Vibrational spectra have been obtained with IR and Raman spectroscopy and the optical activity of the CILs has been recorded for these methods exploiting the differential absorption ΔA by means of vibrational circular dichroism (VCD), and the differential scattering $\Delta d\sigma$, by means of Raman optical activity (ROA), of circularly polarized radiation.[20] Figure 1 shows the recorded spectra.

For the principle of ROA see the Review article of Parchaňský et al.[21] IR and VCD spectra have been recorded with a Bruker Tensor 27/ PMA 50 combination for a thin CIL layer of maximal 6 μm thickness. For Raman and ROA spectra, a self-made spectrometer[22] was utilized and spectra have been recorded in backward scattering geometry. For the scattering experiments, the CILs were contained in a spinning capillary to reduce artefacts. Compared to routine measurements of, for example, small organic molecules as neat liquids or in solution, the acquisition for CILs was challenging. In the case of IR/VCD, difficulties arose because of the strong absorption of the CILs around 1600 cm^{-1}. High laser powers were chosen for Raman/ROA because of the weak scattering of the CILs. The samples were moved slightly off-focus to reduce artefacts.

Careful and slow pipetting was necessary to prohibit the formation of small air bubbles in the sample; which can otherwise easily occur as a result of the CILs' high viscosities. Successful acquisition with both techniques was achieved and the spectra are discussed in more detail below.

It can be seen from Figure 1 that IR and VCD spectra only marginally differ for the three CILs in the small spectral window available. The IR technique VCD is able to discriminate between the two absolute configurations of each amino acid used in the CILs, but its use to differentiate between the CILs is limited. Raman spectra for the CILs differ clearly, especially in the region between 200 and 1200 cm^{-1}, even though the common counterion, Emim, dominates because of its strong scattering cross-sections. Clearly distinct spectra for the three CILs can be obtained by analyzing the differential scattering of left and right circularly polarized light with the ROA setup. As a consequence, we base our discussion on the ROA spectra.

There are several differences between the ROA spectra of the CILs and the corresponding solvated amino acids (see Supporting Information), which provide highly valuable information about the structure and the dynamics of the system. To analyze these spectra in more detail, we applied a combination of high-level calculations encompassing both static and dynamic methods.

As a first step towards a better understanding of the ROA of CILs, calculations for the system with the smallest amino acid for one enantiomer, that is, [L-Ala][Emim], were performed. The resulting theoretical spectra (Figure S17) indicate that a larger cluster of ions has to be considered to obtain a meaningful insight into the system.

[*] Dr. P. Oulevey, Dr. B. Varnholt, Prof. Dr. T. Bürgi
Department of Physical Chemistry, University of Geneva
Quai Ernest-Ansermet 30, 1211 Geneva (Switzerland)
E-mail: patric.oulevey@unige.ch
Dr. S. Luber
Department of Chemistry, University of Zurich
Winterthurerstrasse 190, 8057 Zurich (Switzerland)
Supporting information and the ORCID identification number(s) for the author(s) of this article can be found under http://dx.doi.org/10.1002/anie.201605792.

 © 2016 Wiley-VCH Verlag GmbH & Co. KGaA, Weinheim

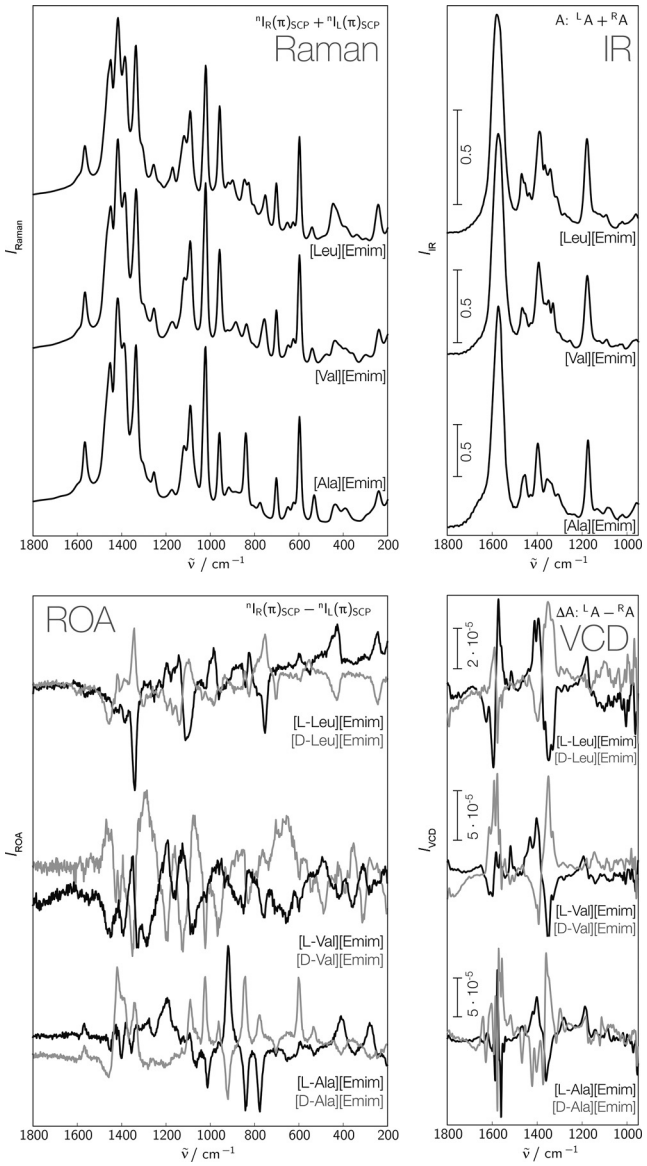

Figure 1. Raman and ROA (left), and IR and VCD (right) spectra of [Ala][Emim], [Val][Emim], and [Leu][Emim]. The spectra are shown as recorded, no modifications have been applied to the data. ROA and VCD spectra are shown for both the L (black) and D (gray) enantiomers for each CIL. The measured CILs were highly viscous and showed fluorescence. During ROA measurements the spinning capillary wobbled slightly around its rest position. Baseline distortions and discrepancies of relative intensities for L/D CIL pairs in those spectra are most likely due to those measurement conditions.

Molecular dynamics (MD) simulations are a powerful tool to investigate the nature and dynamics of the strong interactions between the anions and cations, as well as between the anions themselves through the formation of hydrogen bonds in an ensemble of molecules.[11,23,24] We therefore performed a Born–Oppenheimer MD simulation with Kohn–Sham density functional theory as the electronic structure method (DFT-MD; see Supporting Information for more information). The focus of the analysis of the DFT-MD trajectory lay on the change of dihedral angles that describe the ions' conformation and are therefore accountable for changes in the ROA spectrum. Four dihedral angles were selected, defining the orientation of: the ethyl and methyl group with respect to the Emim's ring plane, and the NH_2 and COO^- group in the L-alaninate ions.

The orientation of the Emim's ethyl group shows an interesting behavior within this chiral environment. To elucidate this in more detail, a dihedral angle was defined such that the ethyl group is in the Emim's ring plane at 0° and 180°. At ± 90° the ethyl group is oriented perpendicular to the plane, and is pointing either downwards (−) or upwards (+). Figure 2 (top) highlights this dihedral angle, as well as the counts how often a specific angle was found throughout the DFT-MD.

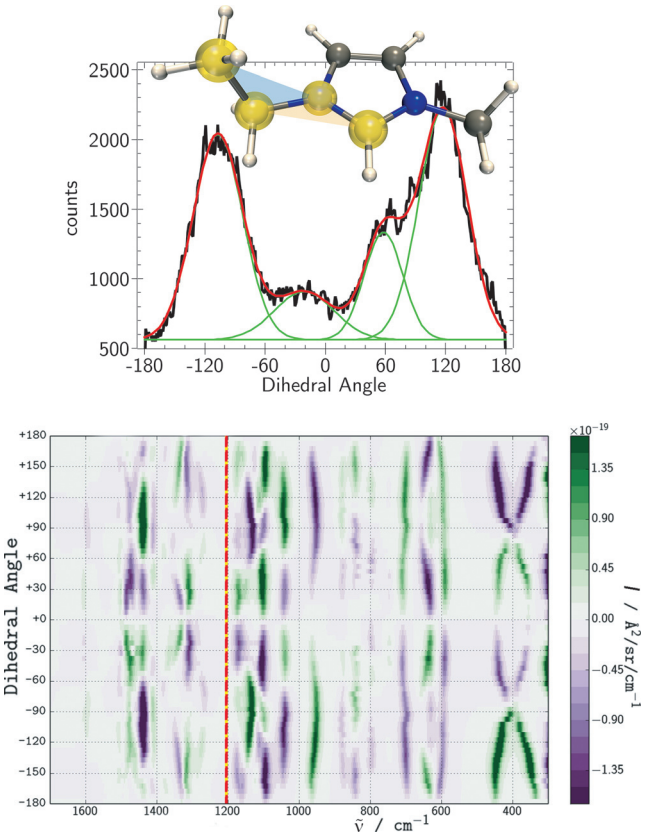

Figure 2. Top: Counts (black line) for the dihedral angle (defined in the Emim molecule shown) obtained from DFT-MD. The red line shows the fitting of four Gaussian curves (green lines). Weightings of the fitted curves are from left to right: 36.1, 9.6, 14.9, and 39.5%. Bottom: 2D plot of ROA spectra as a function of dihedral angle obtained for a complete rotation of the ethyl group in Emim. Positive values are shaded in green, negative values in violet.

In the absence of a chiral environment the distribution of angles is symmetrical around 0°. A fitting of the orientations, the Gaussian curves (green in Figure 2), shows that on the contrary, the distribution is uneven. Chirality is thus induced into Emim, since different transiently chiral conformations (specific ethyl group orientations) are preferred on either side of the ring plane. A comparison between the experiment and calculations of two bands in the Raman spectrum which are very sensitive to the orientation of the ethyl group confirmed

 © 2016 Wiley-VCH Verlag GmbH & Co. KGaA, Weinheim

the distribution obtained from the DFT-MD (see Figures S9 and S12).

The simulation indicates that in the CIL, on average, the Emim adopts a chiral structure, which should leave its trace in the ROA spectra. Two spectral regions were therefore investigated in more detail. The first encompasses the low-wavenumber bands around 300 and 400 cm^{-1} because they were very pronounced in the experimental spectra of the CILs, but not present in the ROA spectrum of the solvated and deprotonated L-alanine (see Figure S1). The second region of interest is the one between 1300 and 1600 cm^{-1} because of its discrepancy between the [L-Ala][Emim] and [D-Ala][Emim] spectra.

To analyze a potential impact of the Emim's transient chirality, we used snapshots of the DFT-MD simulation to make an approximate mean spectrum.[25] Due to the size of the present system and the limited computational resources, we had to restrict ourselves to a low number of frames. Recently, considerable improvements have been made for the snapshot selection of solvated systems.[26,27] In contrast to solvated systems, where one molecule is surrounded by the solvent, in the present system of interacting ions, all molecules in the box have to be considered in the frame selection. Nevertheless, a similar frame selection can be used. We present a simplistic method to extend the weighting procedure of frames.

The selection method consists of a few easily applicable steps. After the definition of dihedral angles (d, as the four defined above) present in the molecules (M^d) of the DFT-MD simulation, the variation of these dihedral angles is analyzed during the DFT-MD run.

Figure 3 explains the procedure for one dihedral angle d. A detailed description of the procedure can be found in the Supporting Information.

If more than one dihedral angle d is analyzed in the system under investigation—which is the case in the present study where four dihedral angles of interest have been defined above—it is sufficient to repeat this procedure for each dihedral angle. A final vector **v** with weights is then simply the sum of those four $\mathbf{v}^d$ vectors. The method is described in more details in the Supporting Information.

With this tool at hand, the three highest weighted snapshots were selected. Figure 4 shows the Raman and ROA spectra of [L-Ala][Emim] of the predictions and the experiment. Two sets of predicted spectra are shown: for the highest weighted snapshot alone, and for the mean spectra of the three most relevant snapshots.

An overall very satisfying agreement with experiment could be achieved, in particular in view of the minimal number of snapshots taken into account.

The predicted and measured Raman spectra match impressively well. ROA predictions are more delicate, nonetheless wide spectral regions could be reproduced down to small pattern details. Three bands assigned to L-Ala around 780, 830, and 920 cm^{-1} have, with respect to the Emim bands, too low intensity. It can be assumed that these bands related to L-Ala gain in intensity, while others attributed to Emim contributions or the Ala-Emim-interactions get more canceled out, the more snapshots are considered. The dihedral

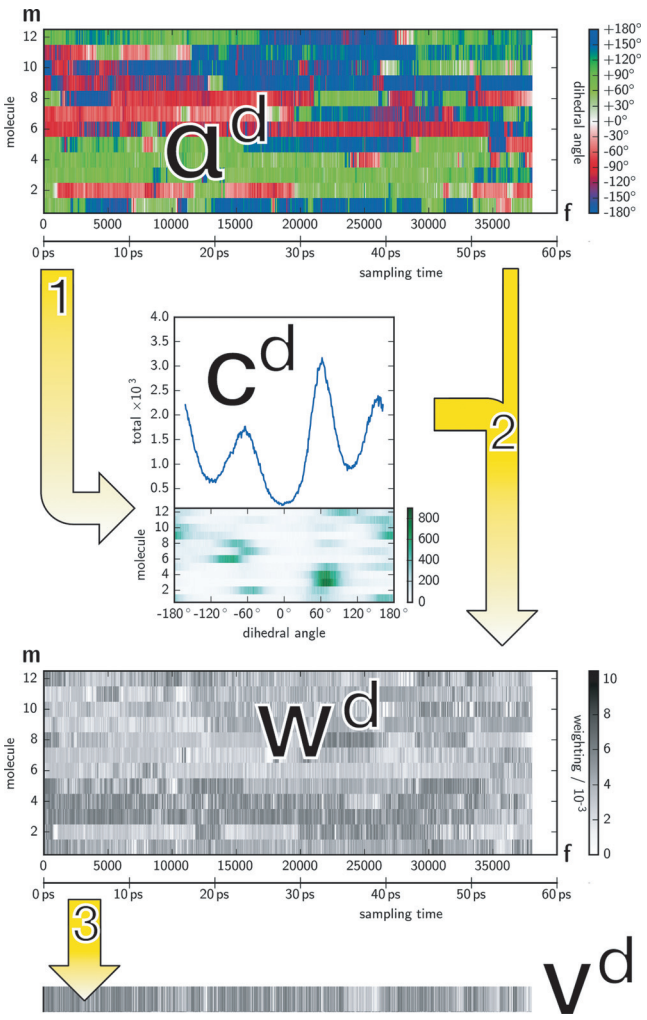

Figure 3. Calculation of weights ($\mathbf{w}^d$) from MD data of dihedral angle d. Example for dihedral angle defining the NH_2 orientation in L-Ala. The top plot shows the dihedral angles ($\boldsymbol{\alpha}^d$) of all L-Ala ions throughout the DFT-MD. From the frequency of occurrence in $\boldsymbol{\alpha}^d$ the counts versus dihedral angle plot ($\mathbf{c}^d$), in the middle, can be obtained. A weighting ($\mathbf{w}^d$) is attributed to each frame by combining $\boldsymbol{\alpha}^d$ and $\mathbf{c}^d$. Finally, a vector $\mathbf{v}^d$ is obtained. The vector elements are the summed weights over all molecules m (12 in this example). A detailed description of the procedure can be found in the Supporting Information.

angles count plots for L-Ala (see Figure S19) show higher confinement to certain orientations than the confinement of the Emim's ethyl group. This ethyl group is thus more easily found to be in different positions and therefore cancels out much more.

An astonishing correlation between predicted and measured ROA spectra can be seen around 400, and between 1200 and 1300 cm^{-1}.

As for the two regions of interest for potential influence of the Emim's induced chirality (at 300/400 cm^{-1} and 1300–1600 cm^{-1}), the snapshot calculations proved helpful as for their decomposition into contributions originating from the L-alaninate ions, the Emim ions, and their interaction (see Figures S21 to S23). In the low-wavenumber region, all three fractions contribute with roughly the same intensities. Around 1300 to 1600 cm^{-1} the L-alaninates give a small

 © 2016 Wiley-VCH Verlag GmbH & Co. KGaA, Weinheim

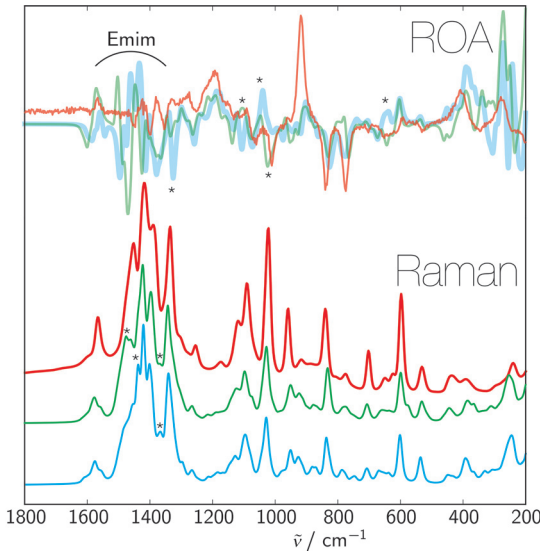

Figure 4. The experimentally observed (red) and predicted (blue and green) Raman (bottom) and ROA (top) spectra of [L-Ala][Emim]. The blue lines correspond to the most relevant snapshot and the green to the arithmetic mean of the three most relevant snapshots according to the method of selection described. Asterisks mark peaks where the inclusion of two more snapshots improved the agreement to experiment.

rather stable contribution, whereas the added intensities from Emim ions and their interaction with L-alaninates are much stronger and subject to large variation in the three snapshots. To predict this region more accurately, a higher number of snapshots would be necessary, which is out of the scope of this work. The high impact of the ions' interaction let us to assume that observed discrepancies in experimental spectra between [L-Ala][Emim] and [D-Ala][Emim] could be due to different experimental conditions and/or sample composition (for example, solvent residues).

In conclusion, we could doubtlessly evidence a perturbation of equilibrium of the enantiomeric forms of the achiral counterion Emim in the chiral environment of the L form of alanine ions. ROA spectra proved to be a suitable technique to clearly differentiate between CILs of different amino acids. The combination of these kinds of optical activity measurements in conjunction with selected computational methods represents a powerful tool for the analysis of highly interacting systems. Getting this kind of insight is crucial for the understanding and design of novel CILs—also with respect to the role of CILs in asymmetric synthesis. The present results suggest that the choice not only of the chiral, but also of the achiral ion is important for CILs used for asymmetric synthesis.

Acknowledgements

Financial support from the University of Geneva is acknowledged.

Keywords: density functional theory · ionic liquids · molecular dynamics · optical activity · Raman spectroscopy

How to cite: *Angew. Chem. Int. Ed.* **2016**, *55*, 11787–11790
Angew. Chem. **2016**, *128*, 11962–11966

[1] J. S. Wilkes, M. J. Zaworotko, *J. Chem. Soc. Chem. Commun.* **1992**, 965–967.
[2] Y. Chauvin, L. Mussmann, H. Olivier, *Angew. Chem. Int. Ed. Engl.* **1995**, *34*, 2698–2700; *Angew. Chem.* **1995**, *107*, 2941–2943.
[3] K. R. Seddon, *J. Chem. Technol. Biotechnol.* **1997**, *68*, 351–356.
[4] P. Wasserscheid, W. Keim, *Angew. Chem. Int. Ed.* **2000**, *39*, 3772–3789; *Angew. Chem.* **2000**, *112*, 3926–3945.
[5] K. K. Laali, *Synthesis* **2003**, 1752.
[6] K. R. Seddon, *Nat. Mater.* **2003**, *2*, 363–365.
[7] M. Schmitkamp, D. Chen, W. Leitner, J. Klankermayer, G. Franciò, *Chem. Commun.* **2007**, 4012–4014.
[8] H. Weingärtner, *Angew. Chem. Int. Ed.* **2008**, *47*, 654–670; *Angew. Chem.* **2008**, *120*, 664–682.
[9] K. Ghandi, *Green Sustainable Chem.* **2014**, *4*, 44–53.
[10] J. B. Rollins, B. D. Fitchett, J. C. Conboy, *J. Phys. Chem. B* **2007**, *111*, 4990–4999.
[11] B. Kirchner, O. Hollóczki, J. N. Canongia Lopes, A. A. H. Pádua, *Wiley Interdiscip. Rev. Comput. Mol. Sci.* **2015**, *5*, 202–214.
[12] C. Baudequin, J. Baudoux, J. Levillain, D. Cahard, A.-C. Gaumont, J.-C. Plaquevent, *Tetrahedron: Asymmetry* **2003**, *14*, 3081–3093.
[13] K. Fukumoto, M. Yoshizawa, H. Ohno, *J. Am. Chem. Soc.* **2005**, *127*, 2398–2399.
[14] J. Ding, D. W. Armstrong, *Chirality* **2005**, *17*, 281–292.
[15] B. Ni, Q. Zhang, A. D. Headley, *Green Chem.* **2007**, *9*, 737–739.
[16] K. Bica, P. Gaertner, *Eur. J. Org. Chem.* **2008**, 3235–3250.
[17] D. Chen, M. Schmitkamp, G. Franciò, J. Klankermayer, W. Leitner, *Angew. Chem. Int. Ed.* **2008**, *47*, 7339–7341; *Angew. Chem.* **2008**, *120*, 7449–7451.
[18] C. P. Kapnissi-Christodoulou, I. J. Stavrou, M. C. Mavroudi, *J. Chromatogr. A* **2014**, *1363*, 2–10.
[19] M. Vasiloiu, P. Gaertner, R. Zirbs, K. Bica, *Eur. J. Org. Chem.* **2015**, 2374–2381.
[20] L. A. Nafie, *Vibrational Optical Activity*, Wiley, Chichester, **2011**.
[21] V. Parchaňský, J. Kapitán, P. Bouř, *RSC Adv.* **2014**, *4*, 57125–57136.
[22] W. Hug, G. Hangartner, *J. Raman Spectrosc.* **1999**, *30*, 841–852.
[23] W. Zhao, F. Leroy, B. Heggen, S. Zahn, B. Kirchner, S. Balasubramanian, F. Müller-Plathe, *J. Am. Chem. Soc.* **2009**, *131*, 15825–15833.
[24] S. Luber, M. Iannuzzi, J. Hutter, *J. Chem. Phys.* **2014**, *141*, 094503.
[25] K. H. Hopmann, K. Ruud, M. Pecul, A. Kudelski, M. Dračínský, P. Bouř, *J. Phys. Chem. B* **2011**, *115*, 4128–4137.
[26] S. T. Mutter, F. Zielinski, P. L. A. Popelier, E. W. Blanch, *Analyst* **2015**, *140*, 2944–2956.
[27] S. T. Mutter, F. Zielinski, J. R. Cheeseman, C. Johannessen, P. L. A. Popelier, E. W. Blanch, *Phys. Chem. Chem. Phys.* **2015**, *17*, 6016–6027.

Received: June 15, 2016
Published online: August 24, 2016

 © 2016 Wiley-VCH Verlag GmbH & Co. KGaA, Weinheim